J Solid State Electrochem (2014) 18:2505–2512
DOI 10.1007/s10008-014-2510-3

ORIGINAL PAPER

Co_3O_4/SiO_2 nanocomposites for supercapacitor application

Gomaa A. M. Ali · Osama A. Fouad · Salah A. Makhlouf · Mashitah M. Yusoff · Kwok Feng Chong

Received: 25 April 2014 / Accepted: 7 May 2014 / Published online: 18 May 2014

Abstract In this study, Co_3O_4/SiO_2 nanocomposites have been successfully synthesized by citrate–gel method by utilizing SiO_2 matrix for Co_3O_4 embedment. Spectroscopy analyses confirm the formation of high crystalline Co_3O_4 nanoparticles; meanwhile, microscopy findings reveal that the Co_3O_4 nanoparticles are embedded in SiO_2 matrix. Electrochemical properties of the Co_3O_4/SiO_2 nanocomposites were carried out using cyclic voltammetry (CV), galvanostatic charge–discharge, and electrochemical impedance spectroscopy (EIS) in 5 M KOH electrolyte. The findings show that the charge storage of Co_3O_4/SiO_2 nanocomposites is mainly due to the reversible redox reaction (pseudocapacitance). The highest specific capacitance of 1,143 F g^{-1} could be achieved at a scan rate of 2.5 mV s^{-1} in the potential region between 0 and 0.6 V. Furthermore, high-capacitance retention (>92 %) after 900 continuous charge–discharge tests reveals the excellent stability of the nanocomposites. It is worth noting from the EIS measurements that the nanocomposites have low ESR value of 0.33 Ω. The results manifest that Co_3O_4/SiO_2 nanocomposites are the promising electrode material for supercapacitor application.

Keywords Supercapacitor · Energy storage · Electrochemistry · Nanocomposites · Cobalt oxide

Introduction

Supercapacitors, which are also known as ultracapacitors or electrochemical capacitors, are the energy storage devices that possess high power density (10 kW kg^{-1}), which can be fully charged or discharged in seconds [1]. In terms of their performance, they can strategically fill in the gap between conventional capacitors and batteries to give better energy and power performance. The potential applications of supercapacitors vary from household electronic products to emergency doors in Airbus A380 planes [2, 3] owing to their excellent energy and power performance. Nonetheless, the energy performance of supercapacitors is still far below as compared to that of batteries. Various research efforts have been attempted in order to enhance the energy performance of the supercapacitors. The energy density of a supercapacitor is given as 0.5 CV^2, where C is the capacitance and V is the operating voltage. Maximizing capacitance value in a supercapacitor is a key factor in enhancing energy performance. Electrode material plays a vital role in this context. The supercapacitors electrode material can be categorized into carbon-based materials (activated carbon, carbon nanotubes, graphene, fullerene, and etc.) [4–7], transition metal oxides (MnO_2, V_2O_5, Fe_2O_3, NiO, CuO, $Co(OH)_2$, Co_3O_4, and etc.) [8–14] and conductive polymers (polyaniline, polypyrrole,

Electronic supplementary material The online version of this article (doi:10.1007/s10008-014-2510-3) contains supplementary material, which is available to authorized users.

G. A. M. Ali · M. M. Yusoff · K. F. Chong (✉)
Faculty of Industrial Sciences & Technology, Universiti Malaysia Pahang, 26300, Gambang, Kuantan, Pahang, Malaysia
e-mail: ckfeng@ump.edu.my

G. A. M. Ali
Chemistry Department, Faculty of Science, Al-Azhar University, Assiut 71524, Egypt

O. A. Fouad
Central Metallurgical Research and Development Institute, CMRDI, P.O. Box 87, Helwan 11421, Egypt

S. A. Makhlouf
Physics Department, Faculty of Science, Assiut University, Assiut 71516, Egypt

S. A. Makhlouf
Deanship of Scientific Research, Al Imam Mohammad Ibn Saud Islamic University (IMSIU), Riyadh 11463, Saudi Arabia

and etc.) [15, 16]. Among all electrode materials, transition metal oxides are often preferred, owing to their low internal resistance that contributes to high power output. Furthermore, different oxidation states of the transition metal oxides could contribute to high pseudocapacitance in the system. They are particularly favored for supercapacitor application due to their cost advantages over noble metal oxides such as RuO_2.

Among all transition metal oxides, Co_3O_4 is a promising electrode material for supercapacitor application by virtue of its high theoretical specific capacitance (3,560 F g^{-1}) [17, 18], reversible surface redox reaction, low cost, and environmental friendliness [14, 19]. Various surface morphologies of Co_3O_4 such as nanoparticles, nanowires, and layered structure [14, 17, 18, 20–22] have been reported for supercapacitor application as the charge storage phenomenon is directly associated with surface properties. However, the reported specific capacitance values for Co_3O_4 are still far below its theoretical value. Therefore, integrated multi-component structure is proposed to provide synergistic effect on energy storage process. For instance, $Co_3O_4/RuO_2 \cdot xH_2O$, $Co_3O_4@MnO_2$, and $Co_3O_4@Pt@MnO_2$ nanocomposites have been developed with enhanced electrochemical performance [23–26]. However, all the literature reports focus on the integration between Co_3O_4 and other metal or metal oxides. To the best of our knowledge, the integration of Co_3O_4 with non-metal oxide for supercapacitor application has not been reported yet.

Herein, we report the fabrication of Co_3O_4/SiO_2 nanocomposites as electrode material for supercapacitor application. It has been proven that SiO_2 could increase the specific capacitance of carbon substrate [27]. SiO_2 is chosen as the non-metal oxide matrix for Co_3O_4 embedment in order to uniformly disperse Co_3O_4 nanoparticles and the electrochemical properties of the nanocomposites are studied.

Experimental section

Sample preparation

The Co_3O_4/SiO_2 nanocomposites were prepared as described in our previous report [28]. Briefly, 13.5 g cobalt chloride (Riedel deHaen, UK, 98 %), 1.85 mL of tetraethyl silicate (Merck, Germany, 99 %), and 1.6 g of citric acid (Adwic, Egypt, 33 %) were dissolved in absolute ethanol (Analar, BDH, 99.8 %), and ultrasonicated for 30 min. The hydrolysis of tetraethyl silicate was done by adding bidistilled water (1:3 volume ratio) into the alcoholic mixture and the pH of the mixture was adjusted to 5. The mixture was heated at 60 °C with continuous stirring for 3 h. A slightly blue gel was obtained and dried in an oven at 80 °C for 24 h. Finally, the dried sample was calcined at 400 °C for 3 h to obtain Co_3O_4 crystallites embedded in SiO_2 matrix.

Sample characterization

Phase identification, and crystallinity of the nanocomposites were studied using an x-ray diffractometer (XRD; Philips PW1700, Netherlands) equipped with an automatic divergent slit. Diffraction pattern was obtained using Cu–K_α radiation (λ=0.15418 nm) and a graphite monochromator in the 2θ range from 10 to 90 °. Infrared spectrum was measured in the range 400–4,000 cm^{-1} using a Fourier transform infrared spectrometer (FTIR; JASCO–480 Plus, Japan). The sample was prepared by KBr disc method. The morphology and elemental analyses of the nanocomposites were investigated using a field emission scanning electron microscope (FESEM; JEOL–JSM–7800 F, Japan), equipped with energy dispersive x-ray analysis (EDX).

Electrochemical measurements

For electrochemical measurements, Co_3O_4/SiO_2 electrode was prepared with a final composition (weight percentage) of 80 % Co_3O_4/SiO_2, 15 % carbon black (Alfa Aesar), and 5 % polytetrafluoroethylene (Aldrich, 60 %). The mixture was casted on nickel foam (Goodfellow) and dried at 60 °C for 30 min. After drying, the coated mesh was uni-axially pressed (5 t) and the weight of the active material was determined by a microbalance. Three-electrode electrochemical system was set up: Co_3O_4/SiO_2 electrode as working electrode, Ag/AgCl (CH Instrument) as reference electrode, and Pt wire (CH Instrument) as counter electrode. Electrochemical data were collected using an electrochemical workstation (AUTOLAB PGSTAT30, Netherlands) equipped with frequency response analyzer. Cyclic voltammetry (CV) tests were performed in the potential range between 0 and 0.6 V vs. Ag/AgCl with scan rates from 2.5 to 30 mV s^{-1}. Galvanostatic charge–discharge tests were performed at different current densities from 1 to 5 A g^{-1}. Electrochemical impedance spectroscopy (EIS) data were collected from 100 kHz to 10 mHz, at open circuit potential with a.c. amplitude of 10 mV. KOH (5 M) was used as the electrolyte throughout all electrochemical measurements.

Results and discussion

Crystal structure and phase analyses

Figure 1 shows the XRD pattern of Co_3O_4/SiO_2 nanocomposites and it can be seen that all the diffraction peaks are related to Co_3O_4 phase (ICDD card # 00–009–0418), suggesting the formation of pure crystalline Co_3O_4 nanoparticles. Diffraction peaks (Fig. 1 insets) were fitted using Lorentzian line shapes for accurate determination of apparent crystallite

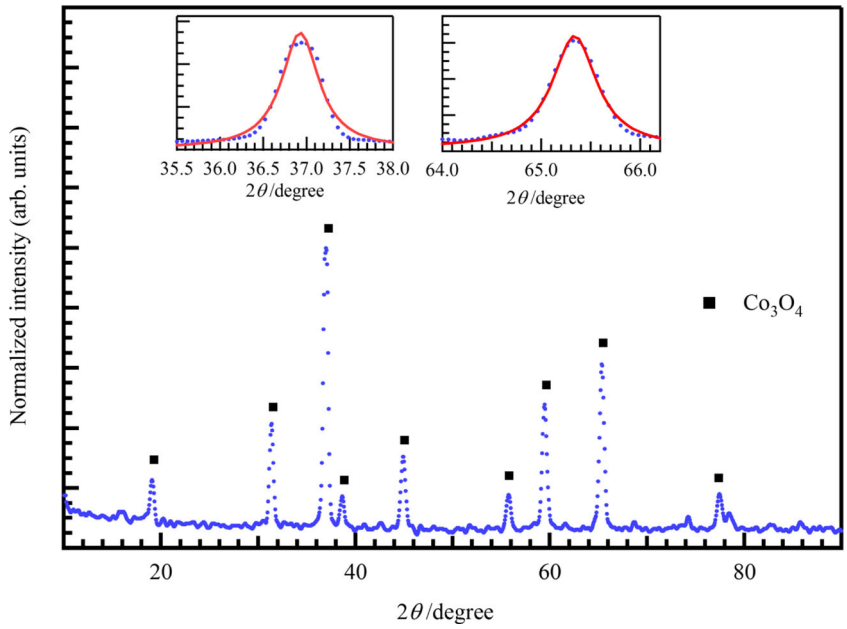

Fig. 1 XRD pattern of Co_3O_4/SiO_2 nanocomposite. The *insets* are zoomed view for some peaks; the *solid lines* are the Lorentzian fitting

size and lattice constant. According to Scherrer formula [29], the apparent crystallite size of Co_3O_4 was calculated to be 26 nm with lattice constant and volume of 0.808 nm and 0.527 nm^3, respectively. The values are slightly larger than those of bulk Co_3O_4 due to surface relaxation usually observed for such nanoparticles [30].

Further information about the chemical structure of Co_3O_4/SiO_2 nanocomposites was obtained from FTIR data shown in Fig. 2. The FTIR bands at 460 and 1,090 cm^{-1} can be assigned to the asymmetric stretching vibration of the bond Si–O–Si in the SiO_4 tetrahedron [30] within SiO_2 matrix. The weak intensity band at 840 cm^{-1} can be attributed to the stretching of non-bridging oxygen atoms in Si–OH bond [28, 30, 31]. Additionally, the absorption bands at 3,440 and 1,635 cm^{-1} correspond to the O–H stretching and bending vibrations, respectively. These observations suggest the presence of absorbed water molecules within SiO_2 matrix. Strong absorption bands can be seen at 560 and 660 cm^{-1}, due to the vibrations of Co–O stretching in Co_3O_4 [30, 31].

The crystalline Co_3O_4 nanoparticles are distributed evenly in SiO_2 matrix, as shown in the FESEM image (Fig. 3a). The findings match with our previous TEM observations [28, 30] of the Co_3O_4 nanoparticles embedded in SiO_2 matrix. Figure 3b shows the EDX data and the Co_3O_4/SiO_2 weight ratio was calculated to be 94.8:5.2. Figure 3c shows the Gaussian fitting of the mean particle size distribution obtained from FESEM image. The obtained mean particle size is 16.5 nm, which is consistent to that obtained from XRD analysis.

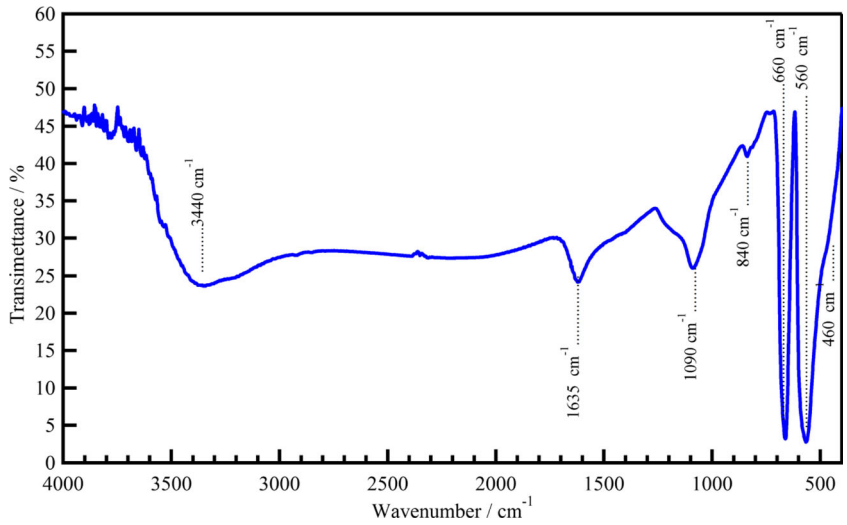

Fig. 2 FTIR spectrum of Co_3O_4/SiO_2 nanocomposite

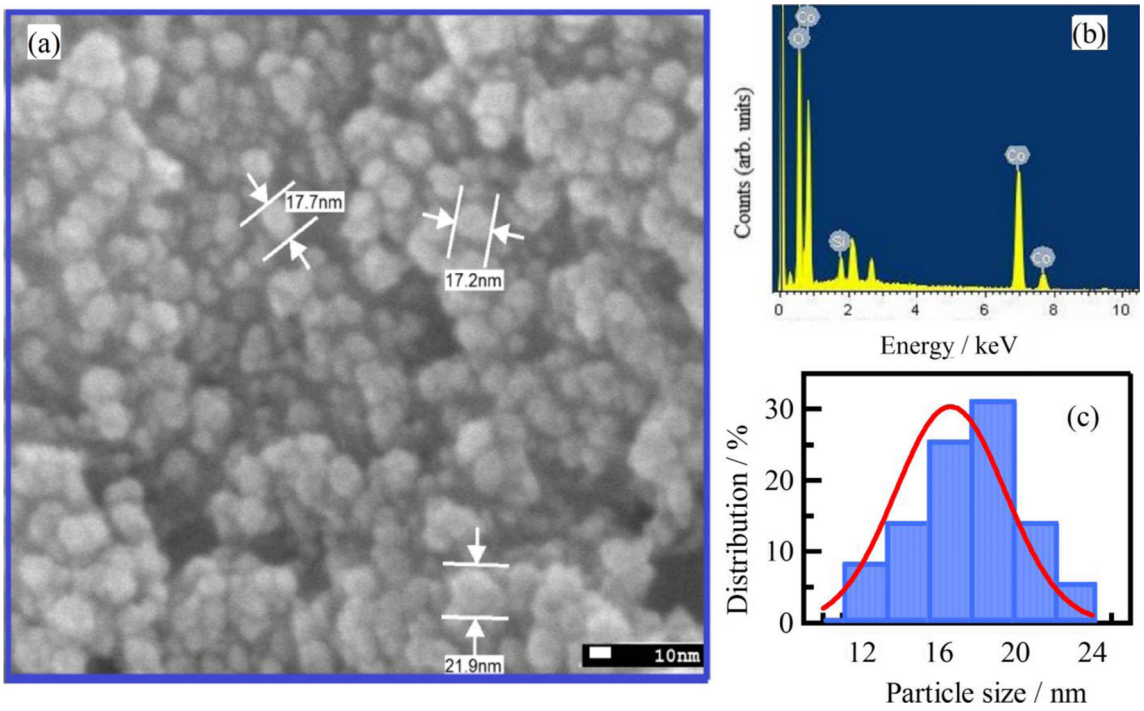

Fig. 3 **a** FESEM image, **b** EDX analysis, and **c** particles size distribution for Co_3O_4/SiO_2 nanocomposite (the *solid line* is the Gaussian fitting)

Electrochemical studies

The charge storage properties of Co_3O_4/SiO_2 electrode were evaluated by CV, galvanostatic charge–discharge and EIS. Figure 4a shows the CV curves of Co_3O_4/SiO_2 electrode in 5 M KOH under different scan rates. It can be seen from the CV curves that Co_3O_4/SiO_2 electrode exhibits pseudocapacitance behavior with two pair of reversible redox peaks. The reversible redox reactions are as follows [17, 20]:

$$Co_3O_4 + OH^- + H_2O \leftrightarrows 3\,CoOOH + e^- \quad (1)$$

$$CoOOH + OH^- \leftrightarrows CoO_2 + H_2O + e^- \quad (2)$$

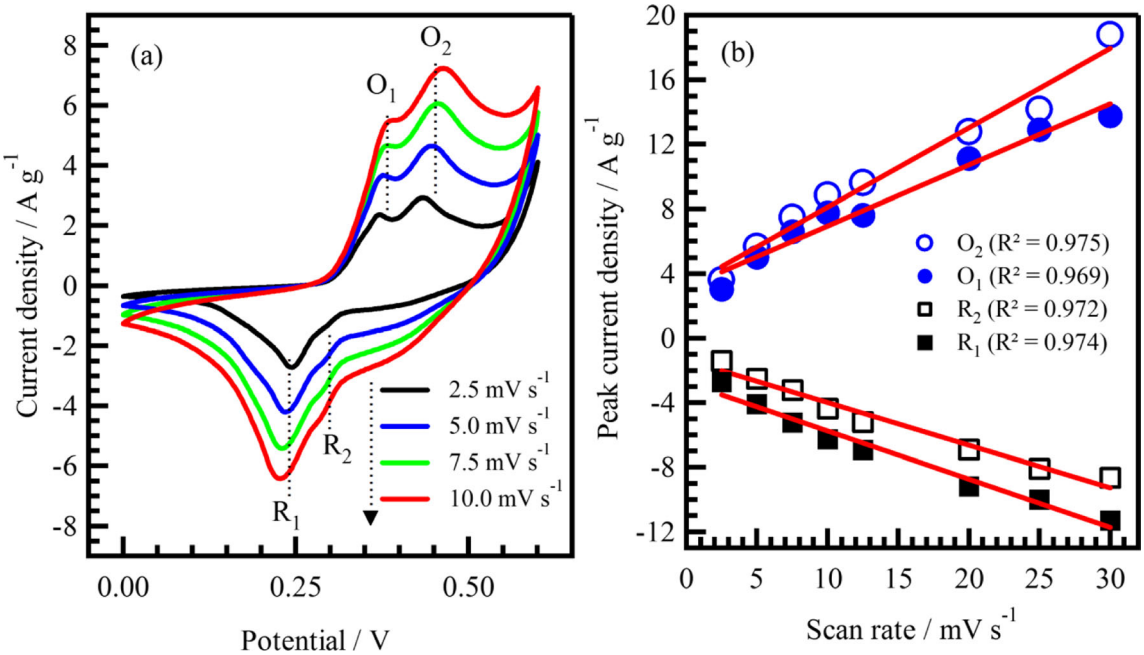

Fig. 4 **a** Cyclic voltammetry at different scan rates and **b** peak current densities versus scan rate for Co_3O_4/SiO_2 electrode in 5 M KOH

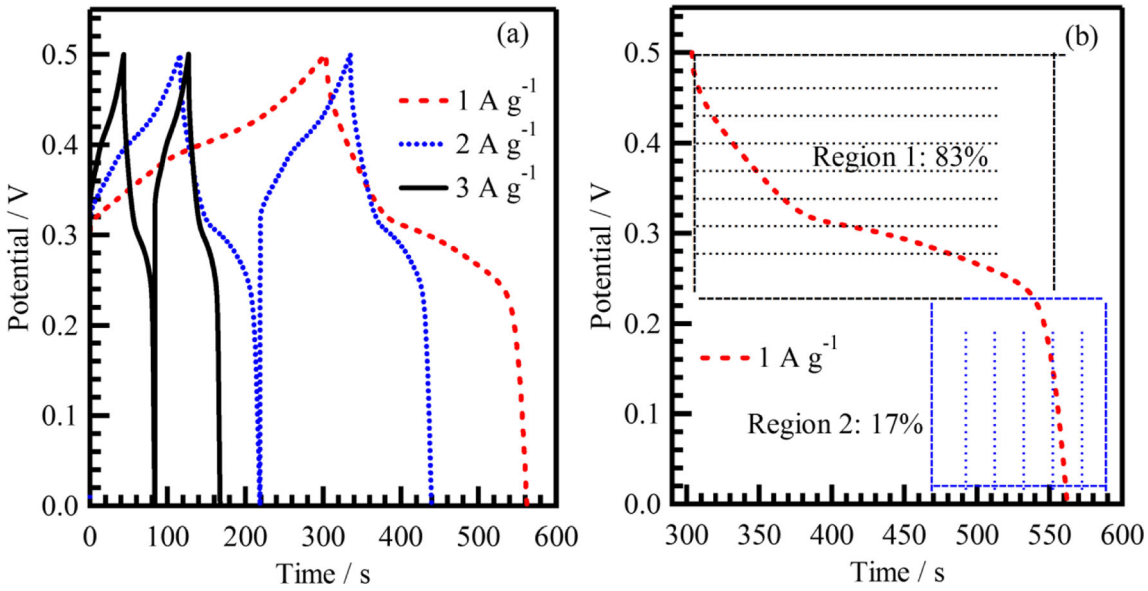

Fig. 5 **a** Galvanostatic charge–discharge curves for Co_3O_4/SiO_2 electrode at various current densities and **b** distribution of pseudocapacitance and electrical double layer capacitance contribution to the capacitance value of Co_3O_4/SiO_2 electrode at 1 A g^{-1} in 5 M KOH

The first redox peaks (O_1/R_1) corresponding to Co^{2+}/Co^{3+} are easily identified at 0.38:0.22 V; the second redox peaks (O_2/R_2) corresponding to Co^{3+}/Co^{4+} occur at 0.46:0.28 V. However, the R_2 reduction peaks are elusive as they just appear as the shoulder of R_1 reduction peaks. Additionally, with an increase in the scan rate, the anodic (O_1, O_2) and cathodic (R_1, R_2) peaks shift to higher and lower potentials, respectively. The peak current densities of Co_3O_4/SiO_2 electrode at different scan rates are summarized in Fig. 4b. Linear relationship between peak current density and scan rate could be observed, indicating the occurrence of surface redox reaction for Co_3O_4/SiO_2 electrode.

To assess the feasibility of Co_3O_4/SiO_2 electrode in the application of supercapacitor, galvanostatic charge–discharge tests were performed at various current densities (Fig. 5a). The shape of the charge–discharge curves is independent of the current density thereby indicating that the Co_3O_4/SiO_2 electrode is suitable for the application of supercapacitor. The discharge curve of Co_3O_4/SiO_2 electrode can be divided into two regions (Fig. 5b), corresponding to pseudocapacitance (region 1) and electrical double layer capacitance (region 2). Region 1 (0.22–0.50 V) with slope variation, contributes 83 % while region 2 (below 0.22 V) with linear slope, contributes only 17 % of the total capacitance. Obviously, large percentage of the specific capacitance in Co_3O_4/SiO_2 electrode is contributed by the reversible redox reactions (pseudocapacitance), as suggested from CV data.

The specific capacitance of Co_3O_4/SiO_2 electrode with respect to scan rate and current density are summarized in Fig. 6. The calculation method can be found in the Supplementary Data. The CV data of Co_3O_4/SiO_2 electrode shows the highest specific capacitance of 1,143 F g^{-1} at a scan rate of 2.5 mV s^{-1}. Apparently, the Co_3O_4/SiO_2 in this study has relatively high specific capacitance value as compared to that of the previous reported values (Table 1) for Co_3O_4 nanocomposites. This could be ascribed to the even distribution of Co_3O_4 nanoparticles in SiO_2 matrix, renders facile electrolyte penetration in the matrix and better surface utilization of the active material for Faradaic reactions. Control experiment had been conducted on Co_3O_4/SiO_2 nanocomposites with higher SiO_2 loading (40 %) to investigate the effect of SiO_2 towards charge storage in nanocomposites (Supplementary data Fig. S1). It shows lower specific capacitance at higher SiO_2 loading, possibly due to lower electroactive material in the nanocomposites. In addition, the

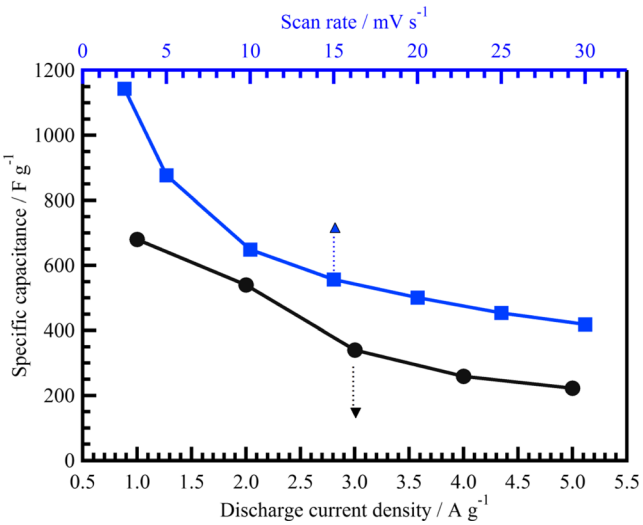

Fig. 6 Specific capacitance as a function of discharge current density (left vs. bottom) and scan rate (left vs. top) for Co_3O_4/SiO_2 electrode

Table 1 Comparison of reported specific capacitance with Co_3O_4/SiO_2 nanocomposites

Material	Specific capacitance (F g^{-1})	
	Cyclic voltammetry (5 mV s^{-1})	Charge–discharge (1 A g^{-1})
$CoMoO_4$ [32]	117	–
Co_3O_4–MnO_2 [25]	419	–
Co_3O_4 [17]	742.3	–
$MnCo_2O_4$ [33]	–	349.8
$NiCo_2O_4$ [34]	–	372
$Co_3O_4/RuO_2 \cdot xH_2O$ [23]	–	642
Co_3O_4/SiO_2 (this work)	*876*	*679*

specific capacitance of Co_3O_4/SiO_2 electrode is dependent of the scan rate as the specific capacitance increases at a lower scan rate. At lower scan rate, the OH^- ions could diffuse into the inner pores of SiO_2 matrix and more OH^- ions are in contact with the Co_3O_4 nanoparticles that are embedded in the matrix, contributing to higher feasible redox reactions as shown in Eqs. 1 and 2. On the other hand, the specific capacitance values of Co_3O_4/SiO_2 electrode derived from galvanostatic charge–discharge are lower than those from CV data. It could be attributed to the low surface accession by OH^- ions under high discharge current density conditions.

Utilization efficiency of the Co_3O_4/SiO_2 electrode had been calculated by comparing the highest attained specific capacitance with the theoretical value. It was calculated as 29.3 %, higher than the reported value for Co_3O_4 nanoparticles (17.5 %) [17], which can be understood as higher surface utilization of Co_3O_4 nanoparticles in SiO_2 matrix. The electrochemical cycling stability is a crucial factor for the supercapacitor application. Figure 7 shows the cycling stability test for Co_3O_4/SiO_2 electrode at a current density of 7 A g^{-1}. High current density is selected for cycling stability test in order to reflect the practical viability of the electrode material for supercapacitor application. It can be noticed that the capacitance retention remains stable (>92 %) up to 900 cycles and only drops to 80.5 % at the 1,000th cycle. This value is higher than that reported for pure Co_3O_4 (65 % after 1,000 cycles and 74 % after 500 cycles) [20, 35], indicating better electrochemical stability of the Co_3O_4/SiO_2 nanocomposites in this work. Such high-capacitance retention suggests that the Co_3O_4/SiO_2 nanocomposites are the good electrode material for supercapacitor application.

The EIS data was analyzed with Nyquist plot. It shows the frequency response at the electrode/electrolyte interface and is a profile of imaginary component (Z'') of the impedance against the real component (Z'). The Nyquist plot of Co_3O_4/SiO_2 electrode (Fig. 8) features a semicircle at high frequency followed by a near 45 ° line at low frequency. The EIS data were analyzed by the CNLS fitting method based on a Randles equivalent circuit, as depicted in Fig. 8 inset, where R_s and R_{ct} are solution and charge transfer resistances, respectively. C_{dl} and C_{ps} represent double layer capacitance and pseudocapacitance, respectively. The interfacial diffusive resistance (Warburg) is designated as W. The solution resistance (R_s) or better known as equivalent series resistance (ESR) is a combination of ionic resistance of electrolyte, intrinsic resistance of active material, and contact resistance of the active material/current collector interface. The low ESR value (0.33 Ω) in this study suggests the good conductivity of Co_3O_4/SiO_2 electrode which contributes to higher redox current. The relatively higher C_{ps} value (258.51 mF) as compared to that of C_{dl} value (0.289 mF) support the galvanostatic charge–discharge findings that the main storage mechanism in the Co_3O_4/SiO_2 electrode is mainly based on Faradaic reaction (pseudocapacitance). The Warburg impedance at low frequency is due to the OH^- ions diffusion within the SiO_2 matrix. All the above–mentioned results demonstrate that Co_3O_4/SiO_2 nanocomposites have good frequency response with low

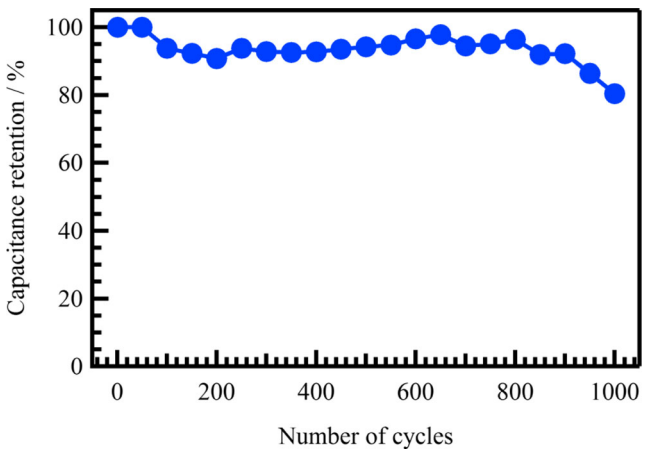

Fig. 7 Cycling stability for Co_3O_4/SiO_2 electrode measured at 7 A g^{-1}

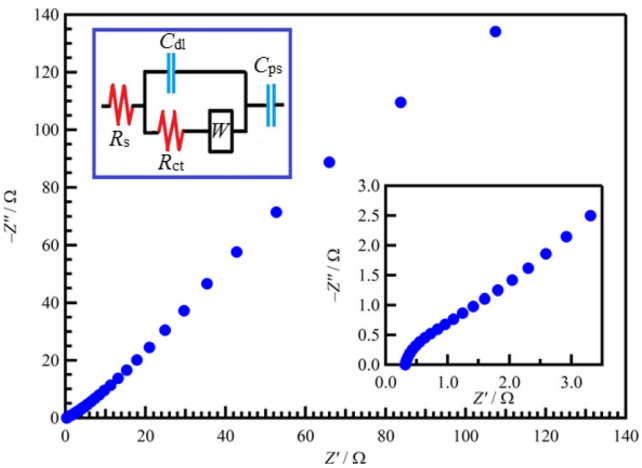

Fig. 8 Nyquist plot of Co_3O_4/SiO_2 electrode. The *insets* are the equivalent circuit and the impedance at high frequency region

impedance and are suitable to be used as electrode material for supercapacitor application.

Conclusions

The present work reports the integration of Co_3O_4 with non-metal oxide in energy storage application. High crystalline Co_3O_4 nanoparticles are embedded and distributed evenly in SiO_2 matrix, using citrate–gel method. The obtained Co_3O_4/SiO_2 nanocomposites show excellent charge storage properties (1,143 F g^{-1} at 2.5 mV s^{-1}; 679 F g^{-1} at 1 A g^{-1}), together with excellent cycling stability, which are attributed to the facile electrolyte penetration in SiO_2 matrix and better Co_3O_4 electroactive surface utilization for redox reactions. Such excellent charge storage properties with low ESR value render Co_3O_4/SiO_2 nanocomposites as promising electrode material for energy storage application.

Acknowledgments KF Chong and co-workers would like to acknowledge the funding from the Ministry of Education Malaysia in the form of MTUN–COE grant RDU121212 and RDU121213.

References

1. Conway BE (1999) Electrochemical supercapacitors scientific fundamentals and technological applications. Kluwer Academic/Plenum Press, New York
2. Martin W, Brodd RJ (2004) What are batteries, fuel cells, and supercapacitors. Chem Rev 104(10):4245–4269
3. Patrice S, Gogotsi Y (2008) Materials for electrochemical capacitors. Nat Mater 7:845–854
4. Kim M-H, Yang J-H, Kang Y-M, Park S-M, Han JT, Kim K-B, Roh KC (2014) Fluorinated activated carbon with superb kinetics for the supercapacitor application in nonaqueous electrolyte. Colloids Surf A 443:535–539
5. Wei S, Kang WP, Davidson JL, Huang JH (2008) Supercapacitive behavior of CVD carbon nanotubes grown on Ti coated Si wafer. Diam Relat Mater 17(4–5):906–911
6. Liu C, Yu Z, Neff D, Zhamu A, Jang BZ (2010) Graphene-based supercapacitor with an ultrahigh energy density. Nano Lett 10(12): 4863–4868
7. Okajima K, Ikeda A, Kamoshita K, Sudoh M (2005) High rate performance of highly dispersed C60 on activated carbon capacitor. Electrochim Acta 51(5):972–977
8. Lee M-T, Chang J-K, Hsieh Y-T, Tsai W-T, Lin C-K (2010) Manganese oxide thin films prepared by potentiodynamic electrodeposition and their supercapacitor performance. J Solid State Electrochem 14(9):1697–1703
9. Qu QT, Shi Y, Li LL, Guo WL, Wu YP, Zhang HP, Guan SY, Holze R (2009) $V_2O_5 \cdot 0.6H_2O$ nanoribbons as cathode material for asymmetric supercapacitor in K_2SO_4 solution. Electrochem Commun 11(6): 1325–1328
10. Kulal PM, Dubal DP, Lokhande CD, Fulari VJ (2011) Chemical synthesis of Fe_2O_3 thin films for supercapacitor application. J Alloys Compd 509(5):2567–2571
11. Nathan T, Aziz A, Noor AF, Prabaharan SRS (2007) Nanostructured NiO for electrochemical capacitors: synthesis and electrochemical properties. J Solid State Electrochem 12(7–8):1003–1009
12. Li Y, Chang S, Liu X, Huang J, Yin J, Wang G, Cao D (2012) Nanostructured CuO directly grown on copper foam and their supercapacitance performance. Electrochim Acta 85:393–398
13. Yuan C, Yang L, Hou L, Li D, Shen L, Zhang F, Zhang X (2011) Synthesis and supercapacitance of flower-like $Co(OH)_2$ hierarchical superstructures self-assembled by mesoporous nanobelts. J Solid State Electrochem 16(4):1519–1525
14. Meher SK, Rao GR (2011) Ultralayered Co_3O_4 for high-performance supercapacitor applications. J Phys Chem C 115(31):15646–15654
15. Mi H, Zhang X, Yang S, Ye X, Luo J (2008) Polyaniline nanofibers as the electrode material for supercapacitors. Mater Chem Phys 112(1):127–131
16. Jureviciute I, Bruckenstein S (2003) Electrochemical activity of chemically deposited polypyrrole films. J Solid State Electrochem 7(9):554–560
17. Wang X, Sumboja A, Khoo E, Yan C, Lee PS (2012) Cryogel synthesis of hierarchical interconnected macro-/mesoporous Co_3O_4 with superb electrochemical energy storage. J Phys Chem C 116(7): 4930–4935
18. Cheng H, Lu ZG, Deng JQ, Chung CY, Zhang K, Li YY (2010) A facile method to improve the high rate capability of Co_3O_4 nanowire array electrodes. Nano Res 3(12):895–901
19. Meher SK, Rao GR (2011) Effect of microwave on the nanowire morphology, optical, magnetic, and pseudocapacitance behavior of Co_3O_4. J Phys Chem C 115(51):25543–25556
20. Li Y, Huang K, Yao Z, Liu S, Qing X (2011) Co_3O_4 thin film prepared by a chemical bath deposition for electrochemical capacitors. Electrochim Acta 56(5):2140–2144
21. Vijayakumar S, Ponnalagi AK, Nagamuthu S, Muralidharan G (2013) Microwave assisted synthesis of Co_3O_4 nanoparticles for high-performance supercapacitors. Electrochim Acta 106:500–505
22. Xie L, Li K, Sun G, Hu Z, Lv C, Wang J, Zhang C (2012) Preparation and electrochemical performance of the layered cobalt oxide (Co_3O_4) as supercapacitor electrode material. J Solid State Electrochem 17(1): 55–61
23. Liu Y, Zhao W, Zhang X (2008) Soft template synthesis of mesoporous $Co_3O_4/RuO_2 \cdot xH_2O$ composites for electrochemical capacitors. Electrochim Acta 53(8):3296–3304
24. Huang M, Zhang Y, Li F, Zhang L, Wen Z, Liu Q (2014) Facile synthesis of hierarchical $Co_3O_4@MnO_2$ core-shell arrays on Ni foam for asymmetric supercapacitors. J Power Sources 252:98–106
25. Kim SH, Kim YIL, Park JH, Ko JM (2009) Cobalt–manganese oxide–carbon–nanofiber composite. Int J Electrochem Sci 4:1489–1496
26. Xia H, Zhu D, Luo Z, Yu Y, Shi X, Yuan G, Xie J (2013) Hierarchically structured $Co_3O_4@Pt@MnO_2$ nanowire arrays for high-performance supercapacitors. Sci Rep 3:2978–2986
27. Leonard KC, Suyama WE, Anderson MA (2011) Improvement of electrochemical capacitor electrodes using SiO_2 nanoparticles. Electrochim Acta 56(27):10137–10144
28. Fouad OA, Ali GAM, El–Erian MAI, Makhlouf SA (2012) Humidity-sensing properties of cobalt oxide/silica nanocomposites prepared via sol–gel and related routes. Nano 7(5):1250038–1250049
29. Patterson A (1939) The Scherrer formula for x–ray particle size determination. Phys Rev 56(10):978–982
30. Fouad OA, Makhlouf SA, Ali GAM, El–Sayed AY (2011) Cobalt/silica nanocomposite via thermal calcination–reduction of gel precursors. Mater Chem Phys 128(1–2):70–76
31. Esposito S, Turco M, Ramis G, Bagnasco G, Pernice P, Pagliuca C, Bevilacqua M, Aronne A (2007) Cobalt–silicon mixed oxide nanocomposites by modified sol–gel method. J Solid State Chem 180(12): 3341–3350

32. Veerasubramani GK, Krishnamoorthy K, Radhakrishnan S, Kim N-J, Kim SJ (2014) Synthesis, characterization, and electrochemical properties of $CoMoO_4$ nanostructures. Int J Hydrogen Energy 39(10): 5186–5193
33. Li L, Zhang YQ, Liu XY, Shi SJ, Zhao XY, Zhang H, Ge X, Cai GF, Gu CD, Wang XL, Tu JP (2014) One–dimension $MnCo_2O_4$ nanowire arrays for electrochemical energy storage. Electrochim Acta 116:467–474
34. Kuang M, Zhang W, Guo XL, Yu L, Zhang YX (2014) Template-free and large-scale synthesis of hierarchical dandelion-like $NiCo_2O_4$ microspheres for high–performance supercapacitors. Ceram Int. doi:10.1016/j.ceramint.2014.02.099
35. Wang L, Liu X, Wang X, Yang X, Lu L (2010) Preparation and electrochemical properties of mesoporous Co_3O_4 crater-like microspheres as supercapacitor electrode materials. Curr Appl Phys 10(6): 1422–1426